

# Multomics Analysis of Plasma Proteomics and Metabolomics of Steroid Resistance in Childhood Nephrotic Syndrome Using a “Patient-Specific” Approach



Sagar Bhayana<sup>1,8</sup>, Yue Zhao<sup>2,8</sup>, Michael Merchant<sup>3</sup>, Timothy Cummins<sup>3</sup>, Julie A. Dougherty<sup>1</sup>, Yu Kamigaki<sup>1</sup>, Wimal Pathmasiri<sup>4</sup>, Susan McRitchie<sup>4</sup>, Laura H. Mariani<sup>5</sup>, Susan Sumner<sup>4</sup>, Jon B. Klein<sup>3,6,9</sup>, Lang Li<sup>7,9</sup>, William E. Smoyer<sup>1,7,9</sup>, and on behalf of the Pediatric Nephrology Research Consortium<sup>10</sup>

<sup>1</sup>Center for Clinical and Translational Research, Nationwide Children’s Hospital; Columbus, Ohio, USA; <sup>2</sup>Department of Computational Medicine and Bioinformatics, University of Michigan Medical School, Ann Arbor, Michigan, USA; <sup>3</sup>Department of Medicine, Division of Nephrology and Hypertension, University of Louisville; Louisville, Kentucky, USA; <sup>4</sup>Department of Nutrition, Nutrition Research Institute, University of North Carolina at Chapel Hill; Kannapolis, North Carolina, USA; <sup>5</sup>Division of Nephrology, Department of Internal Medicine, Michigan Medicine, Ann Arbor, Michigan, USA; <sup>6</sup>Robley Rex VA Medical Center, Louisville, Kentucky, USA; and <sup>7</sup>Department of Pediatrics, College of Medicine, The Ohio State University, Columbus, Ohio, USA

**Introduction:** Nephrotic syndrome (NS) occurs commonly in children with glomerular disease and glucocorticoids (GCs) are the mainstay treatment. Steroid resistant NS (SRNS) develops in 15% to 20% of children, increasing the risk of chronic kidney disease compared to steroid sensitive NS (SSNS). NS pathogenesis is unclear in most children, and no biomarkers exist that predict the development of pediatric SRNS.

**Methods:** We studied a unique patient cohort with plasma specimens collected before GC treatment, yielding a disease-only sample not confounded by steroid-induced gene expression changes (SSNS  $n = 8$ ; SRNS  $n = 7$ ). A novel “patient-specific” bioinformatic approach merged paired pretreatment and post-treatment proteomic and metabolomic data and identified candidate SRNS biomarkers and altered molecular pathways in SRNS versus SSNS.

**Results:** Joint pathway analyses revealed perturbations in nicotinate or nicotinamide and butanoate metabolic pathways in patients with SRNS. Patients with SSNS had perturbations of lysine degradation, mucin type O-glycan biosynthesis, and glycolysis or gluconeogenesis pathways. Molecular analyses revealed frequent alteration of molecules within these pathways that had not been observed by separate proteomic and metabolomic studies. We observed upregulation of NAMPT, NMNAT1, and SETMAR in patients with SRNS, in contrast to upregulation of ALDH1B1, ACAT1, AASS, ENPP1, and pyruvate in patients with SSNS. Pyruvate regulation was the change seen in our previous analysis; all other targets were novel. Immunoblotting confirmed increased NAMPT expression in SRNS and increased ALDH1B1 and ACAT1 expression in SSNS, following GC treatment.

**Conclusion:** These studies confirmed that a novel “patient-specific” bioinformatic approach can integrate disparate omics datasets and identify candidate SRNS biomarkers not observed by separate proteomic or metabolomic analysis.

*Kidney Int Rep* (2023) 8, 1239–1254; <https://doi.org/10.1016/j.ekir.2023.03.015>

KEYWORDS: biomarker; informatics; MetaboAnalystR; nephrosis; personalized; steroid resistance

© 2023 International Society of Nephrology. Published by Elsevier Inc. This is an open access article under the CC BY-NC-ND license (<http://creativecommons.org/licenses/by-nc-nd/4.0/>).

**Correspondence:** William E. Smoyer, Center for Clinical and Translational Research Abigail Wexner Research Institute at Nationwide Children’s Hospital, Room W303, 700 Children’s Drive, Columbus, Ohio 43205, USA. E-mail: [William.Smoyer@Nationwidechildrens.org](mailto:William.Smoyer@Nationwidechildrens.org); or Lang Li, Department of Biomedical Informatics, College of Medicine, The Ohio State University, 320B Lincoln Tower, 1800 Cannon Dr Columbus, Ohio 43210, USA. E-mail: [Lang.Li@osumc.edu](mailto:Lang.Li@osumc.edu); or Jon B. Klein, 570 S. Preston Street, Room 102S Donald Baxter Research Building, University of Louisville Health Sciences Center, Louisville, Kentucky 40202, USA. E-mail: [jon.klein@louisville.edu](mailto:jon.klein@louisville.edu)

<sup>8</sup>SB and YZ have equal first authorship.

<sup>9</sup>JK, LL, and WS have co-senior authorship.

<sup>10</sup>Members of Pediatric Nephrology Research Consortium are listed in the [Appendix](#).

Received 28 February 2023; accepted 20 March 2023; published online 23 March 2023

NS is a clinical syndrome defined by massive proteinuria ( $>40$  mg/m<sup>2</sup> per hour) with resulting hyperlipidemia, edema, and various renal and extrarenal complications.<sup>1</sup> It results from abnormal glomerular permeability that may be either primary or secondary to systemic disease or exposures, including infections, diabetes, systemic lupus erythematosus, neoplasia, or various drugs.<sup>2</sup> Common pathologic changes in primary NS are minimal change disease, focal segmental glomerulosclerosis, diffuse mesangial sclerosis, and membranous nephropathy,<sup>3</sup> with minimal change disease being the most common cause in children. GCs are the mainstay therapy for these disorders. However, 20% to 30% of children present with or develop GC resistance and 36% to 50% of these children progress to end-stage kidney disease in 10 years.<sup>4</sup> The clinical management of SRNS is challenging because few therapies have been found to be consistently effective and most of the available alternative treatments have significant toxicity.<sup>5</sup> Furthermore, there are no validated biomarkers that distinguish SRNS from SSNS at disease presentation. Identification of biomarkers of SRNS would greatly enhance our ability to develop more effective and safer treatments for pediatric NS.

To bridge this gap, we performed an integrated analysis of plasma proteomics and plasma metabolomics data from pediatric patients with SRNS and SSNS, both before and following initial GC treatment.<sup>6,7</sup> We hypothesized that integration of proteomic and metabolomic data would identify novel NS biomarker candidates not identified by individual proteomics and metabolomics analyses alone. We further hypothesized that analysis of these paired pre-GC-treated and post-GC-treated plasma samples using a novel “patient-specific” approach to large data set analysis would identify molecular pathways associated with steroid resistance (i.e., SRNS), despite individual patients having disparate molecular defects along these pathways. Although such a patient-specific approach for omics data analysis has been developed previously for genomics and transcriptomics data,<sup>8–12</sup> its application to renal disease is new, and the specific integration of proteomic and metabolomic datasets has been very limited.<sup>13,14</sup> Therefore, our studies attempted to use this “patient-specific” approach to integrate plasma proteomics and metabolomics from patients with SRNS and SSNS to identify and compare molecular pathways altered in SRNS versus SSNS.

## METHODS

### Study Approval

All research protocols and consent documents were approved by the institutional review board of Nationwide Children’s Hospital as the coordinating center

(approval numbers IRB07–00400, IRB12–00039, and IRB05–00544), as well as by each of the other participating centers of the Pediatric Nephrology Research Consortium. Paired plasma samples were collected for each patient, with the first sample “pretreatment” at the time of disease presentation before even a single dose of GC, and the second sample “posttreatment” after 6 to 10 weeks of GC therapy when the clinical determination of SSNS versus SRNS had been made by the treating nephrologist. All samples were anonymously coded as stipulated by the Declaration of Helsinki.<sup>15</sup>

### Study Design

Integrated pathway analysis was conducted by using the datasets acquired by previously published research work by our laboratory.<sup>6,7</sup> Grouped and patient-specific analyses were performed to investigate for biomarkers and/or mechanistic insights of steroid resistance. The candidate pathways and the molecules involved were further validated by immunoblotting. See [Figure 1](#) for an overview of the study design.

### Proteomic and Metabolomic Data Analysis

See [Supplementary Methods](#).

### “Patient-Specific” Integrated Pathway Analysis Overview

Altered proteins and metabolites were selected for each patient and then jointly fed into a pathway for an enrichment analysis. Only pathways that were enriched in at least 1 patient were further compared between patients with SSNS and patients with SRNS. To characterize the enrichment of a pathway in patients with SRNS compared to patients with SSNS, a Pathway Group Enrichment Index and a Molecule Group Enrichment Index were calculated. Finally, the false discovery rate (FDR) was calculated jointly for all “patient-specific” pathway analyses. The following are detailed descriptions of these pathway analyses.

### Altered Protein and Metabolite List for Individual Patients

The relative intensity-based absolute quantification values of proteins from 15 paired NS plasma samples (SSNS,  $n = 7$  pairs; SRNS,  $n = 8$  pairs) and relative concentration of metabolites estimated from the same subjects were used for generating protein and metabolite lists. For each patient, the fold change was calculated as the ratio of posttreatment to pretreatment (posttreatment/pretreatment) for each protein and metabolite, and then log<sub>2</sub> transformed to get log<sub>2</sub> fold change (LFC). When checking the LFCs’ distributions of proteins and metabolites for each patient ([Supplementary Figure S1](#)), we observed that LFC =

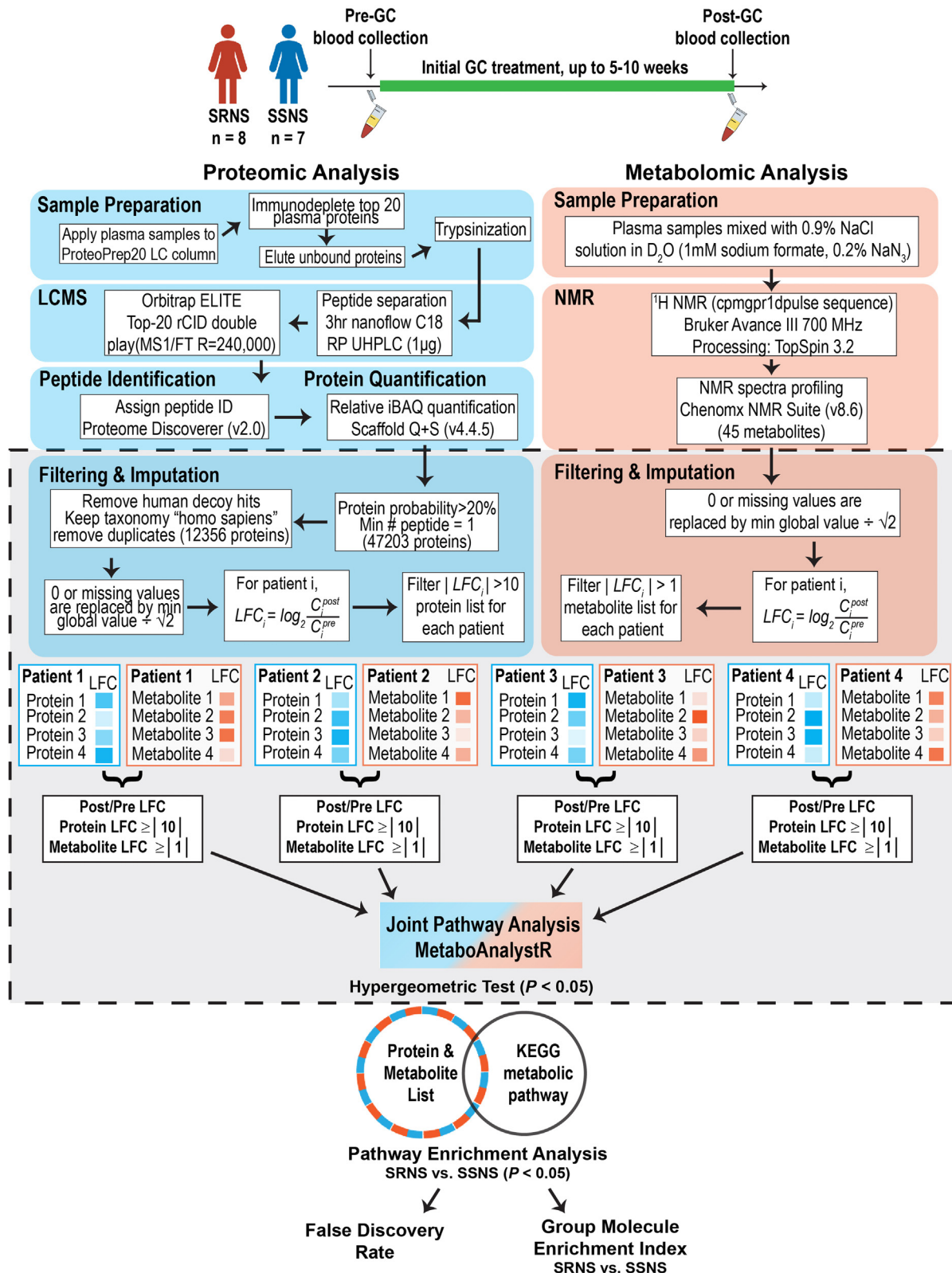


**Figure 1.** Integration of plasma proteomic and metabolomic data from patients with SRNS and patients with SSNS using a “patient-specific” joint pathway analysis. Plasma samples were collected from 7 patients with SSNS and 8 patients with SRNS before and after GC treatment. All 30 samples underwent both proteomic and metabolomic analyses. Then for each patient, proteins and metabolites were selected and jointly fed for enrichment analysis into MetaboAnalystR. Only pathways that were enriched ( $P < 0.05$ ) in at least 1 patient were further compared between SSNS and SRNS patients. To characterize the enrichment of a pathway in patients with SRNS compared to patients with SSNS, 2 Group Enrichment Indexes were calculated (see Methods). Finally, the false discovery rate was calculated jointly for all “patient-specific” pathway analyses. Novel methods for this study are highlighted with the dashed gray box. GC, glucocorticoids; KEGG, Kyoto Encyclopedia of Genes and Genomes; LFC,  $\log_2$  fold change; NMR, Nuclear Magnetic Resonance; SRNS, steroid resistant nephrotic syndrome; SSNS, steroid sensitive nephrotic syndrome.

$\pm 10$  and  $\pm 1$  served best to separate proteins and metabolites, respectively, into 3 groups: 1 unaltered group with LFC approximately 0, and 2 altered groups with large LFCs, while keeping enough proteins and metabolites for pathway enrichment analysis. Altered proteins and metabolites are defined as differentially regulated having increased or decreased expression based on respective LFC cutoffs.

### Pathway Enrichment Analysis

We used the “Joint Pathway Analysis” function in MetaboAnalystR v3.0.3 and exploited KEGG metabolic pathway models to complete the analysis.<sup>16</sup> For each patient, the list of altered proteins with Uniprot protein accession number and altered metabolites with KEGG ID (Supplementary Data Files S1 and S2) were pooled into a single query and were mapped to KEGG metabolic pathways for hypergeometric test. Pathway hypergeometric test  $P$ -value  $< 0.05$  was considered as significant.

### Pathway Group Enrichment Index Calculation

To characterize the enrichment of a pathway in patients with SRNS compared to patients with SSNS, we defined the Pathway Group Enrichment Index as:

$$\left( \frac{\text{Number of SRNS patients with pathway altered}}{\text{Total number of SRNS patients}} - \frac{\text{Number of SSNS patients with pathway altered}}{\text{Total number of SSNS patients}} \right) \times 100\%$$

Using this equation, positive percentages indicated the pathway was frequently altered in patients with SRNS. Conversely, negative percentages indicated that the pathway was frequently altered in patients with SSNS. Pathways with absolute values of Group Enrichment Index  $> 25\%$  were selected to visualize the links between each patient and each molecular pathway in a chord plot (see Figure 2). We chose to investigate the top pathways for patients with SRNS and patients with SSNS with further analyses.

Similarly, for protein and metabolite selection, we defined the Molecule Group Enrichment Index as:

$$\left( \frac{\text{Number of SRNS patients with molecule up regulated post GC treatment}}{\text{Total number of SRNS patients}} - \frac{\text{Number of SSNS patients with molecule up regulated post GC treatment}}{\text{Total number of SSNS patients}} \right) \times 100\%$$

Using this equation, the Molecule Group Enrichment Index represented the enrichment of an upregulated protein or metabolite in patients with SRNS compared to patients with SSNS, with positive percentages indicating enrichment in patients with SRNS and negative percentages indicating enrichment in patients with SSNS. Given the small sample size, we required the absolute value of the Molecule Group Enrichment Index to be at least 30% to consider a molecule as a candidate for validation.

### FDR Determination

The FDR is the expected rate at which features called significant are truly null.<sup>17</sup> If we set the significance level  $\alpha = 0.05$ , then under the null hypothesis, the conditional probability of a false discovery (mistakenly claim an enriched pathway) is  $P=0.05$ . In our study, we controlled the expected proportion of false discoveries among the predicted enriched pathways (Supplementary Data File S3) in 3 scenarios as follows.

**Scenario 1.** If a pathway is enriched more frequently in patients with SRNS (e.g., the nicotinate and nicotinamide metabolism, SSNS = 0, SRNS = 4), we ask the question: “Is this pathway enriched (hypergeometric  $P$ -value  $< 0.05$ ) more frequently in patients with SRNS?” The probability that at least 4 of 8 patients with SRNS are enriched in 1 pathway follows binomial distribution:

$$P_{binom}(n \geq 4 | N = 8, p = 0.05) = 0.000372$$

The probability that at most 0 out of 7 patients with SSNS is enriched in 1 pathway is calculated as:

$$P_{binom}(n \leq 0 | N = 7, P = 0.05) = 0.698$$

The joint probability is:

$$P_{binom}(n \geq 4 | N = 8, p = 0.05) \cdot P_{binom}(n \leq 0 | N = 7, p = 0.05) = 0.000372 \times 0.698 = 0.00026$$



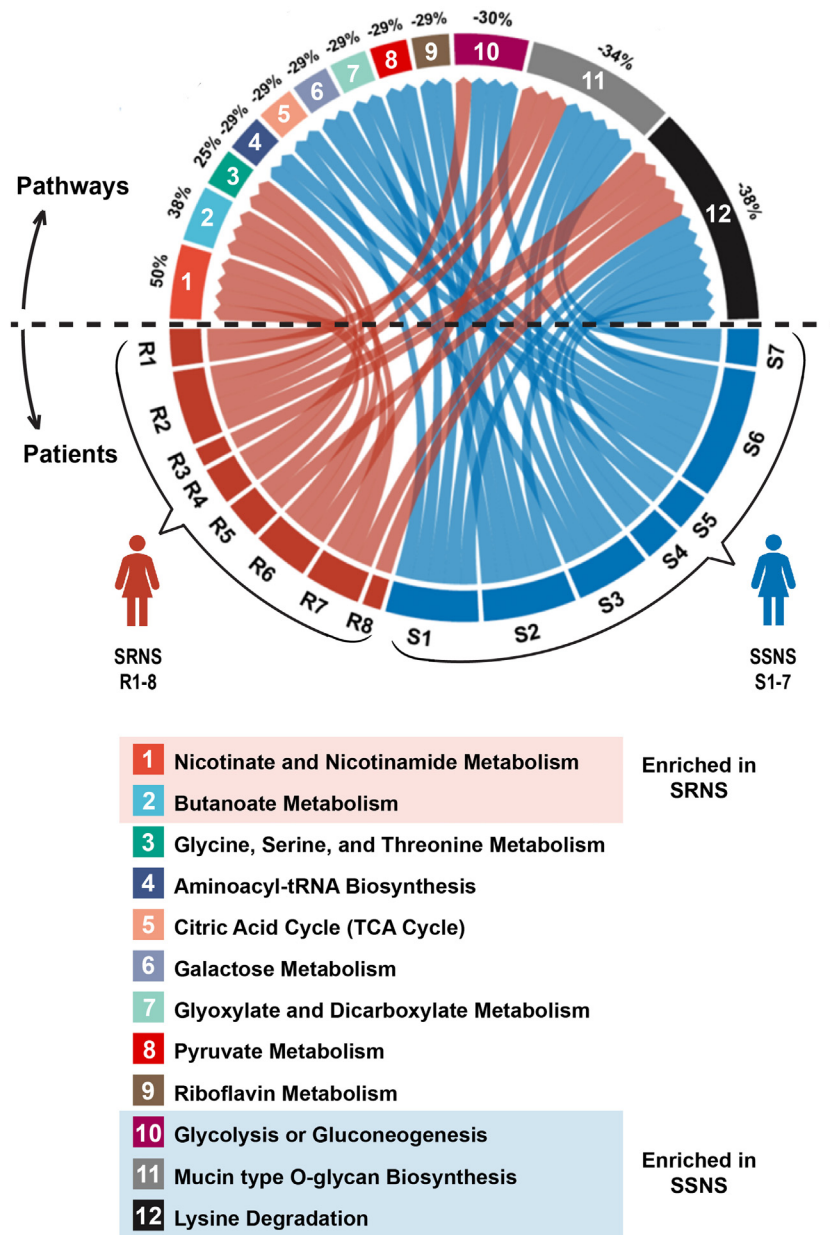


**Figure 2.** Comparison of pathways altered by glucocorticoids in patients with SRNS vs. patients with SSNS using a “patient-specific” analysis of integrated omics. Chord plot represents pathways that were significantly perturbed ( $P < 0.05$ ) by joint pathway analysis for individual patients. R1–R8: 8 patients with SRNS (in red); S1–S7: 7 patients with SSNS (in blue). For example, patient R1 had 2 pathways significantly perturbed: nicotinate and nicotinamide metabolism and mucin type O-glycan biosynthesis. For pathway mucin type O-glycan biosynthesis, 3 patients with SRNS (R1, R2, and R6) and 5 patients with SSNS (S1, S3, S4, S6, and S7) had this pathway activated. The percentages labeled above the pathways are Pathway Group Enrichment Index numbers calculated by

$$\left( \frac{\text{Number of SRNS patients with pathway altered}}{\text{Total number of SRNS patients}} - \frac{\text{Number of SSNS patients with pathway altered}}{\text{Total number of SSNS patients}} \right) \times 100\%$$

, which represents the enrichment of a pathway in patients with SRNS compared to patients with SSNS. Although a total of 34 KEGG metabolic pathways were perturbed in 15 patients, we selected 12 pathways whose Pathway Group Enrichment Index was  $< -25\%$  or  $>25\%$  to show in this chord plot. TCA, tricarboxylic acid cycle.

We have 83 unique metabolic pathways for hypergeometric test. So, the expected proportion of false discoveries is:

$$FDR = 83 \times 0.00026 = 0.022$$

**Scenario 2.** If a pathway is enriched equal times in patients with SRNS and in patients with SSNS (e.g., the glycerolipid metabolism, SSNS = 4, SRNS = 4), we ask the question: “Is this pathway enriched in both groups

of patients?" The probability that at least 4 out of 8 patients with SRNS are enriched in 1 pathway:

$$P_{binom}(n \geq 4 | N = 8, p = 0.05) = 0.000372$$

The probability of at least 4 out of 7 patients with SSNS are enriched in 1 pathway is calculated as:

$$P_{binom}(n \geq 4 | N = 7, P = 0.05) = 0.000194$$

The joint probability is:

$$P_{binom}(n \geq 4 | N = 8, p = 0.05) \cdot P_{binom}(n \geq 4 | N = 7, p = 0.05) = 0.000372 \times 0.000194 = 7.196 \times 10^{-8}$$

We have 83 unique metabolic pathways for hypergeometric test. So, the expected proportion of false discoveries is:

$$FDR = 83 \times 7.196 \times 10^{-8} = 5.97 \times 10^{-6}$$

**Scenario 3.** If a pathway is enriched more frequently in patients with SSNS (e.g., the lysine degradation, SSNS = 7, SRNS = 5), we ask the question: "Is this pathway enriched more frequently in patients with SSNS?" The probability that at most 5 out of 8 patients with SRNS are enriched in 1 pathway:

$$P_{binom}(n \leq 5 | N = 8, p = 0.05) = 1$$

The probability of at least 7 out of 7 patients with SSNS are enriched in 1 pathway is calculated as:

$$P_{binom}(n \geq 7 | N = 7, p = 0.05) = 7.813 \times 10^{-10}$$

The joint probability is:

$$P_{binom}(n \leq 5 | N = 8, p = 0.05) \cdot P_{binom}(n \geq 7 | N = 7, p = 0.05) = 7.813 \times 10^{-10}$$

We have 83 unique metabolic pathways for hypergeometric test. So, the expected proportion of false discoveries is:

$$FDR = 83 \times 7.813 \times 10^{-10} = 6.48 \times 10^{-8}$$

### Principal Component Analysis

The Principal Component Analysis (PCA) was done on the LFC of proteins for proteomics data, LFC of metabolite concentrations for metabolomics data, combined proteomics and metabolomics datasets, and proteins and metabolites mapped to the selected 5 altered pathways. These PCA plots were generated by R package *factoextra* v1.0.7 (<https://www.rdocumentation.org/packages/factoextra/versions/1.0.7>).

### Heatmap Annotated With Clinical Data

To evaluate the trends of LFC of protein abundance and metabolite concentration, the LFC data of each protein or metabolite were centered by subtracting their mean values across 15 patients. Then, the values of each protein and metabolite entry were scaled by dividing the centered values by their standard deviations across 15 patients. These normalized LFCs were used for heat map generation using R package *Complex Heatmap* v2.2.0.

### Immunoblotting

See [Supplementary Methods](#).

### Statistics

All values were presented as mean  $\pm$  standard error of the mean. Statistical analyses were performed using R and GraphPad Prism. Statistically significant differences were determined by Wilcoxon rank sum test. *P*-values less than 0.05 were of significance. For immunoblots, nonparametric Wilcoxon rank sum analyses were conducted for LFC comparison and Kruskal-Wallis tests were used for preabundance and post-abundance comparisons. Tests were 2-tailed, at alpha = 0.05, with *P*-values less than 0.05 considered statistically significant.

## RESULTS

### Integration of Plasma Proteomic and Metabolomic Data From Patients with SRNS and Patients with SSNS using a "Patient-Specific" Joint Pathway Analysis

Integrated pathway analysis was conducted by using previously acquired nuclear magnetic resonance metabolomic and liquid chromatography tandem mass spectrometry proteomic data.<sup>6,7</sup> The analysis workflow is shown in [Figure 1](#). Plasma samples collected from 7 patients with SSNS and 8 patients with SRNS, before and after initial GC treatment were processed for omics and data preprocessing. The SRNS and SSNS patient demographics were reported in a previous study<sup>6</sup> (see [Supplementary Table S1](#)). Briefly, patients were between the ages of 2 and 14 years old ( $8.7 \pm 1.0$  years), with similar pre-GC and post-GC treatment sampling ( $6.0 \pm 0.5$  weeks), and all were steroid-naïve before enrollment. The details of the sample collection, sample preparation, and data acquisition were described previously.<sup>6,7</sup> Clinical information of patients, including laboratory tests and biopsy results are listed in [Supplementary Table S2](#). We reprocessed and reprofiled previous raw nuclear magnetic resonance metabolomic data to increase the number of metabolites for pathway-based integration study, and all 45 metabolites were included in the downstream analysis. Whereas the previous studies were focused on the

discrimination of SRNS from SSNS populations using separate proteomic and metabolomic analyses,<sup>6,7</sup> the current study integrated the previously acquired proteomic and metabolomic datasets using a novel “patient-specific” approach (Figure 1, gray dashed box). Consequently, the relative (to internal standard) concentrations of the metabolites were recalculated (Supplementary Data Files S4a, S4b). For each metabolite, the missing value fractions in pre-GC treatment and post-GC treatment samples were independent of patients of SSNS and those with SRNS (Supplementary Data File S5). For proteomics data, the relative intensity-based absolute quantification values of proteins were subjected to missing value imputation and filtering steps (see Methods section and Supplementary Figure S1A–C). For each patient, the LFC was then calculated as the  $\log_2$  transformed ratio of post-GC treatment level to pre-GC treatment level (posttreatment/pre-treatment) for each protein (Supplementary Data File S3) and metabolite (Supplementary Data File S2). On the basis of distributions of LFCs (Supplementary Figure S2), we included proteins with  $LFC < -10$  or  $> 10$  and metabolites with  $LFC < -1$  or  $> 1$  in the joint pathway analysis. Subsequently, for each patient, the lists of altered proteins and metabolites were combined and mapped to KEGG metabolic pathways for pathway enrichment analysis by using hypergeometric tests (Supplementary Data File S6).

We identified 34 enriched metabolic pathways in patients with SRNS and patients with SSNS based on hypergeometric  $P$ -values  $< 0.05$  (Supplementary Table S3). To determine if specific pathways were enriched more frequently in SRNS versus SSNS, we ranked these 34 pathways by their Pathway Group Enrichment Index percentage, calculated as the frequency of enrichment in SRNS versus SSNS (defined in detail the Methods section). A positive index indicated pathways that were enriched in a greater number of patients with SRNS, and a negative index indicated pathways that were enriched in a greater number of patients with SSNS. For instance, the nicotinate and nicotinamide pathway (also known as the  $NAD^+$  biosynthesis pathway) had a Pathway Group Enrichment Index of 50% (i.e., enriched in 4 of 8 patients with SRNS and 0 of 7 patients with SSNS,  $FDR = 0.022$ ), whereas the lysine degradation pathway had a Group Enrichment Index of  $-37.5\%$  (i.e., enriched in all 7 patients with SSNS and 5 of 8 patients with SRNS,  $FDR < 0.0001$ ).

### Comparison of Pathways Altered by GCs in Patients With SRNS Versus SSNS Using a “Patient-Specific” Analysis of Integrated Omics

Of 34 significantly altered pathways in post-GC treatment, 12 pathways with a Group Enrichment

Index  $< -25\%$  or  $> 25\%$  were used to visualize links between patients and molecular pathways. This cut-off was set to provide a minimum likelihood of the pathway being enriched in patients with SRNS or patients with SSNS (for a detailed explanation, refer to Methods section). A chord plot was then created to link each patient with SRNS (R1–R8 in Figure 2, Supplementary Data File S7) and each patient with SSNS (S1–S7 in Figure 2, Supplementary Data File S7) to each of these 12 enriched molecular pathways. Notably, the chord plot provided a holistic view of the personalized integrated analyses of each patient. For instance, patient R4 with SRNS had 2 pathways (shown by red links) significantly altered after GC treatment as follows: (i) butanoate metabolism, and (ii) glycine, serine, and threonine metabolism; and patient S7 with SSNS had 2 different pathways (shown by blue links) significantly altered after GC treatment as follows: (i) mucin type O-glycan biosynthesis, and (ii) lysine degradation pathway (Figure 2, Supplementary Figure S4). If we count 1 link in the chord plot as a “patient-specific” altered pathway activity, 7 patients with SSNS had 27 activities (shown in blue in Figure 2) in 9 unique molecular pathways significantly perturbed after GC therapy. Notably, the SRNS group had only 18 activities (shown in red) in 6 unique pathways significantly perturbed after GC therapy. This suggests the biologic pathways altered by GC treatment in children with SRNS were not similarly altered by GC treatment in SSNS.

### Comparison of Pathways Suppressed by GCs in Patients With SSNS Versus SRNS

To identify active pathways at baseline that are successfully suppressed by GC treatment in SSNS but not in SRNS, we performed joint pathway analysis on the downregulated proteins ( $\text{Log}_2\text{FC} < -10$ ) and altered metabolites ( $|\text{Log}_2\text{FC}| > 1$ ). Results showed 32 pathways significantly (hypergeometric test,  $P < 0.05$ ) downregulated either in SSNS or SRNS (Supplementary Table S4). Interestingly, 2 pathways were significantly enriched for downregulated molecules by GC treatment in SSNS compared to SRNS ( $FDR < 0.05$ ): phosphatidylinositol signaling system and lysine degradation. The following 3 pathways were enriched for suppression by GC treatment in SSNS and unchanged in SRNS: aminoacyl-tRNA biosynthesis, citrate cycle (tricarboxylic acid cycle), and pyruvate metabolism; but their  $FDR$  was not  $< 0.05$ . These data suggest the hypothesis that these pathways may be related to the disease process that responds to steroids. Further, the following 3 pathways with downregulated molecules were enriched in patients with SRNS and unchanged in patients with SSNS:

glycosaminoglycan biosynthesis – chondroitin sulfate/dermatan sulfate; neomycin, kanamycin, and gentamicin biosynthesis; and starch and sucrose metabolism. These pathways may be related to underlying mechanisms of steroid resistance.

### Principal Component Analysis of Targets from Enriched Pathway Integration Enabled Better Separation of SRNS From SSNS than Analysis of Entire Proteomic Data Alone

No 2 patients had identical pathways enriched, regardless of their being in the SRNS or the SSNS group. On the basis of the directionality of these molecular changes derived from both proteins and metabolites for the 5 pathways enriched, PCA was able to separate the 2 groups of patients with only a moderate degree of overlap, emphasizing that the analysis of integrated multiomic data identified pathways was able to differentiate SRNS from SSNS (Figure 3a). In comparison, a similar PCA plot derived from the entirety of the proteomic and metabolomic data in a population-based analysis was unable to distinctly differentiate SRNS from SSNS, as illustrated by the increased overlap of the SRNS and SSNS ellipses (Figure 3b). In addition, the ellipses for the patient groups were tighter with less intragroup variation for the enriched pathways from the integrated “patient-specific” approach (Figure 3a) as compared to those derived from the entirety of data using a grouped approach (Figure 3b). A protein-only PCA plot demonstrated poor differentiation between the 2 groups (Supplementary Figure S3a), whereas a

metabolites-only PCA plot better differentiated the patient groups (Supplementary Figure S3b).

### Nicotinate and Nicotinamide Metabolism Maps from Patients with SRNS Highlight Extensive “Patient-Specific” Molecular Diversity among Patients with Identical Phenotypes (i.e. SRNS)

We also compared individual molecular pathway maps of patients within the same response group (i.e., SRNS or SSNS) to investigate the molecular diversity underlying GC responses. Figure 4 shows an example of this, where we found that the nicotinate and nicotinamide metabolism pathway was enriched in 4 patients with SRNS (R1, R5, R6, R7); however, the specific molecules altered and the direction of changes were not identical for all patients with SRNS. Additionally, multiple pathway maps could be generated for individual patients (Supplementary Figure S4). These findings highlight the “patient-specific” molecular diversity of these patients within a common pathway, all of whom presented with the identical clinical phenotype of primary SRNS.

### Identification of “Patient-Specific” Molecular Alterations among Pathways Altered in SRNS Versus SSNS

To increase stringency in our selection and to identify a biomarker frequently altered we narrowed our focus from 12 to the top 5 altered pathways (nicotinate and nicotinamide metabolism, butanoate metabolism, glycolysis or gluconeogenesis, mucin type O-glycan biosynthesis, and lysine degradation) that were

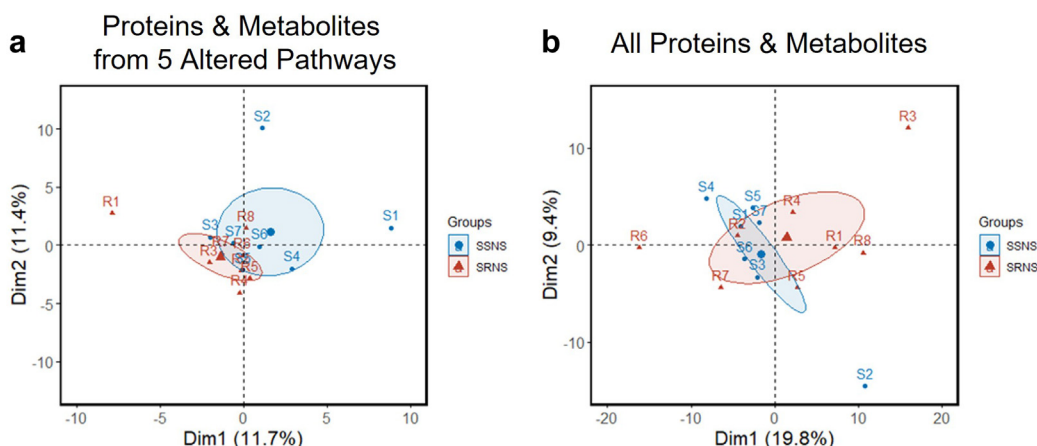


**Figure 3.** Principal component analysis of targets from enriched altered pathway integration enabled better separation of SRNS from SSNS than analysis of integrated data set alone. PCA of the LFCs from (a) the integrated proteins plus metabolites in the 5 altered pathways enriched  $\geq 30\%$  and (b) all proteins and metabolites. The variation explained by each principal component is indicated in parenthesis on the axis label. The small blue dots represent individual patients with SSNS, whereas the small red triangles represent individual patients with SRNS. Each ellipse defines the region that contains 95% of all samples that can be drawn from the underlying Gaussian distribution. The large blue dot and large red triangle represent the group centroids. SRNS, steroid resistant nephrotic syndrome; SSNS, steroid sensitive nephrotic syndrome.



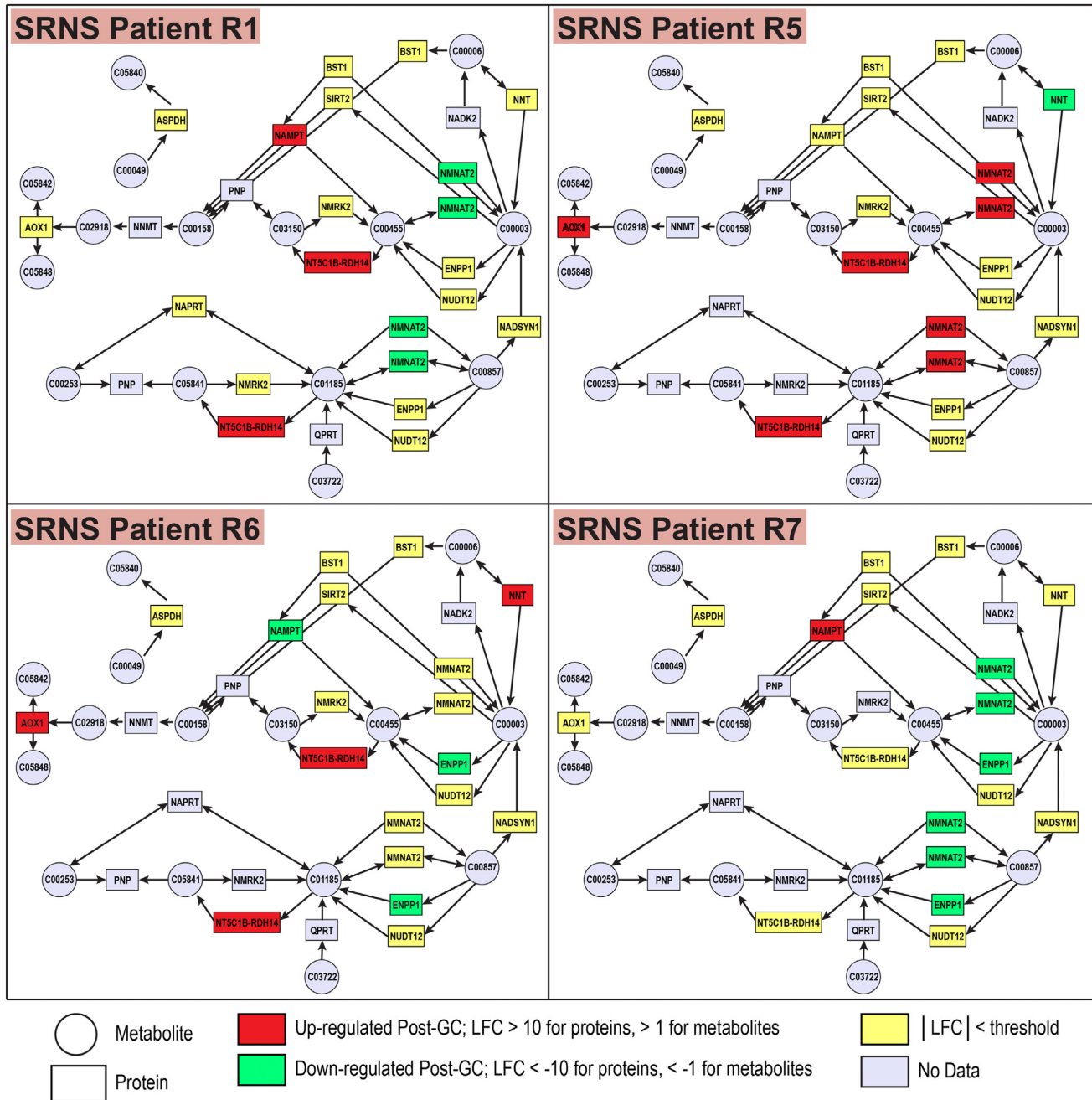


**Figure 4.** Nicotinate and nicotinamide metabolism maps from patients with SRNS highlight extensive “patient-specific” molecular diversity among patients with identical clinical phenotypes. Proteins (rectangles) and metabolites (circles) are mapped with interactions (arrows) for the pathway. Upregulated molecules above the LFC threshold are indicated in red, and downregulated molecules below the LFC threshold are indicated in green. Molecules that changed but were not above the thresholds are indicated in yellow. Molecules with no data are indicated in gray. SRNS, steroid resistant nephrotic syndrome.

dysregulated in at least 3 patients and graphed the relative abundance of the LFCs of the proteins/metabolites in these pathways in a heatmap (Figure 5). Molecules such as NAMPT and NMNAT1 in the nicotinate and nicotinamide metabolism pathway (highlighted with red text in Figure 5 Section #1 at top), together with SETMAR in the lysine degradation pathway (highlighted with red text in Figure 5 Section #12 at the bottom), had more frequent positive LFCs (i.e., protein expression increased in response to GC

treatment) in patients with SRNS versus patients with SSNS. Meanwhile, ENPP1, ALDH1B, AASS, and ACAT1 had less frequent positive LFCs in patients with SRNS (highlighted with blue text in Figure 5).

### Molecule Group Enrichment Index Scores Differentiate Molecules Most Altered in Patients with SSNS Versus SRNS

We next determined the Molecule Group Enrichment Index of the molecules in the 5 chosen pathways in the

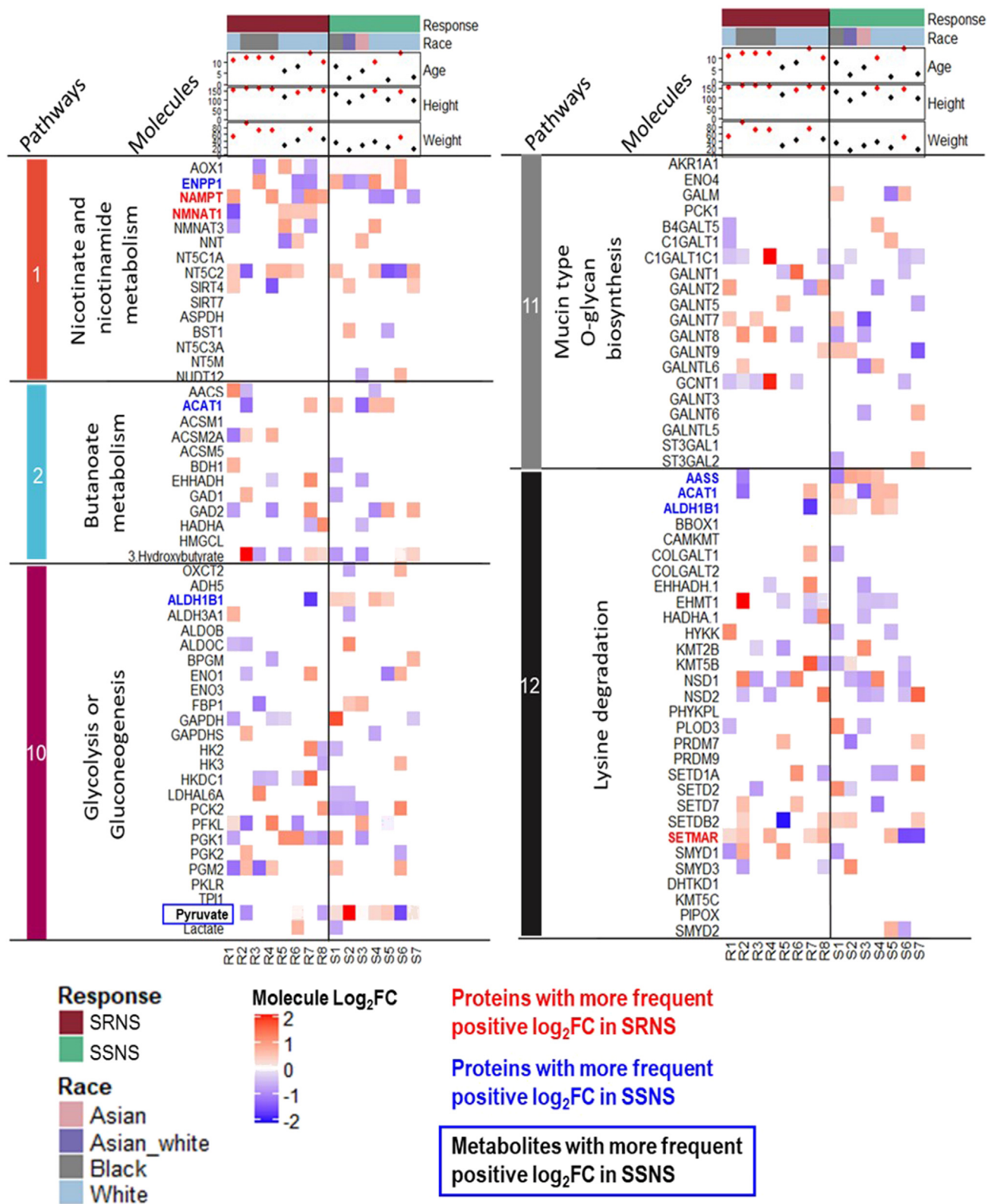


**Figure 5.** Identification of “patient-specific” molecular alterations among pathways altered in patients with SRNS versus SSNS. Heatmap represents LFCs of protein or metabolite LFCs from 15 patients (8 SRNS and 7 SSNS) for the 5 pathways with Pathway Group Enrichment Index values  $\leq -30\%$  or  $\geq 30\%$  (pathways # 1, 2, 10, 11, 12 in Figure 2). Clinical data are plotted at the top. For numeric variables (age, height, and weight), the red dots represent values above the median and the black dots represent values below the median. Based on the frequency of positive LFCs in a group, 10 molecules were selected and were highlighted by red or blue text if more positive LFCs existed in patients with SRNS (red text) and patients with SSNS (blue text). SRNS, steroid resistant nephrotic syndrome; SSNS, steroid sensitive nephrotic syndrome.

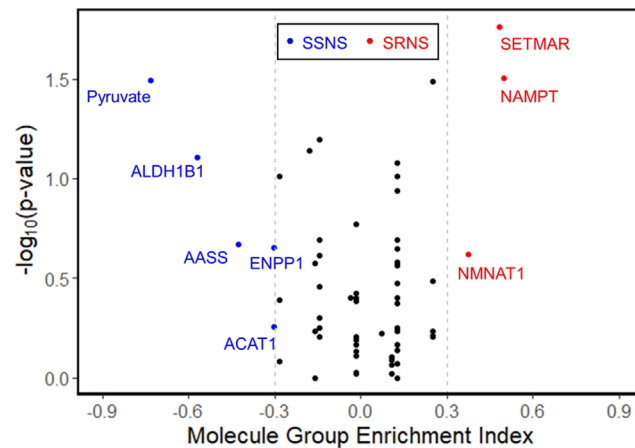


**Figure 6.** Molecule Group Enrichment Index scores differentiate molecules most altered in patients with SSNS versus patients with SRNS. A volcano plot displays all identified plasma proteins and metabolites on the basis of their Molecule Group Enrichment Index, calculated as

$$\left( \frac{\text{Number of SRNS patients with molecule up regulated post GC treatment}}{\text{Total number of SRNS patients}} - \frac{\text{Number of SSNS patients with molecule up regulated post GC treatment}}{\text{Total number of SSNS patients}} \right) \times 100\%$$

This value for each molecule represents the enrichment of an upregulated protein or metabolite in patients with SRNS versus patients with SSNS. The y-axis is the  $P$ -value of Wilcoxon rank sum test between the number of positive LFCs of patients with SRNS and patients with SSNS,  $\log_{10}$  transformed and multiplied by  $-1$ . Given the small sample size, we required the absolute value of the Molecule Group Enrichment Index to be at least 30% for choosing a molecule as a candidate for validation, and we did not set a cut-off for  $P$ -value. A positive index indicates enrichment in patients with SRNS and those molecules enriched with an index  $>30\%$  are shown as red dots, whereas a negative index indicates enrichment in patients with SSNS and those molecules enriched  $< -30\%$  are shown as blue dots. SRNS, steroid resistant nephrotic syndrome; SSNS, steroid sensitive nephrotic syndrome.

patients with SRNS versus patients with SSNS (Figure 6). These analyses revealed that NAMPT, SETMAR, and pyruvate LFC levels showed significant differences between patients with SRNS and patients with SSNS (Wilcoxon rank sum test;  $P$ -value  $< 0.05$ ). Although ALDH1B1, ACAT1, NMNAT1, and ENPP1 had more frequent positive LFCs in either patients with SRNS or patients with SSNS, their differences were not significant. Given the small sample size, we required increasing the stringency of our analysis and narrowed our focus for validation. Of the 77 molecules in the 5 pathways, 8 molecules were thus selected.

Unfortunately, in the previously published grouped analyses<sup>6,7</sup> the small numbers of differentially expressed proteins ( $n = 60$ ) and metabolites ( $n = 3$ ) (Supplementary Figure S5) were not suitable to perform pathway analyses, which confirmed that the integrative multiomics approach provided additional knowledge that could not be revealed by analyses of the separate datasets.

### Confirmation of Changes in Proteins-of-Interest by Immunoblotting

Our integrated pathway analysis approach identified 8 molecules (SETMAR, NAMPT, NMNAT1, pyruvate,

ALDH1B1, AASS, ENPP1, and ACAT1) based on their  $\geq |30\%|$  Molecule Group Enrichment Index and we selected NAMPT, ALDH1B1, and ACAT1 for further validation. We analyzed pre-GC and post-GC treatment plasma from the same patients and performed immunoblotting on all samples to observe the following: (i) average pre-GC and post-GC expression levels, (ii) the change in expression with GC treatment in each patient, and (iii) the LFC in Expression with GC treatment.

ALDH1B1 was readily detected in patient samples, both pre-GC and post-GC treatment (Figure 7a). ALDH1B1 levels were significantly lower ( $P < 0.01$ ) pre-GC in patients with SSNS versus SRNS, demonstrating its potential as a predictive biomarker of SRNS (Figure 7a, left panel). Most patients with SSNS had increased ALDH1B1 levels post-GC treatment, whereas most patients with SRNS showed decreased levels with GC treatment (Figure 7a, middle panel). Aligned with the heatmap in Figure 5, the  $\log_2$  fold change (post-GC treatment/pre-GC treatment) for ALDH1B1 was significantly higher in patients with SSNS versus SRNS ( $P < 0.01$ ; Figure 7a, right panel).



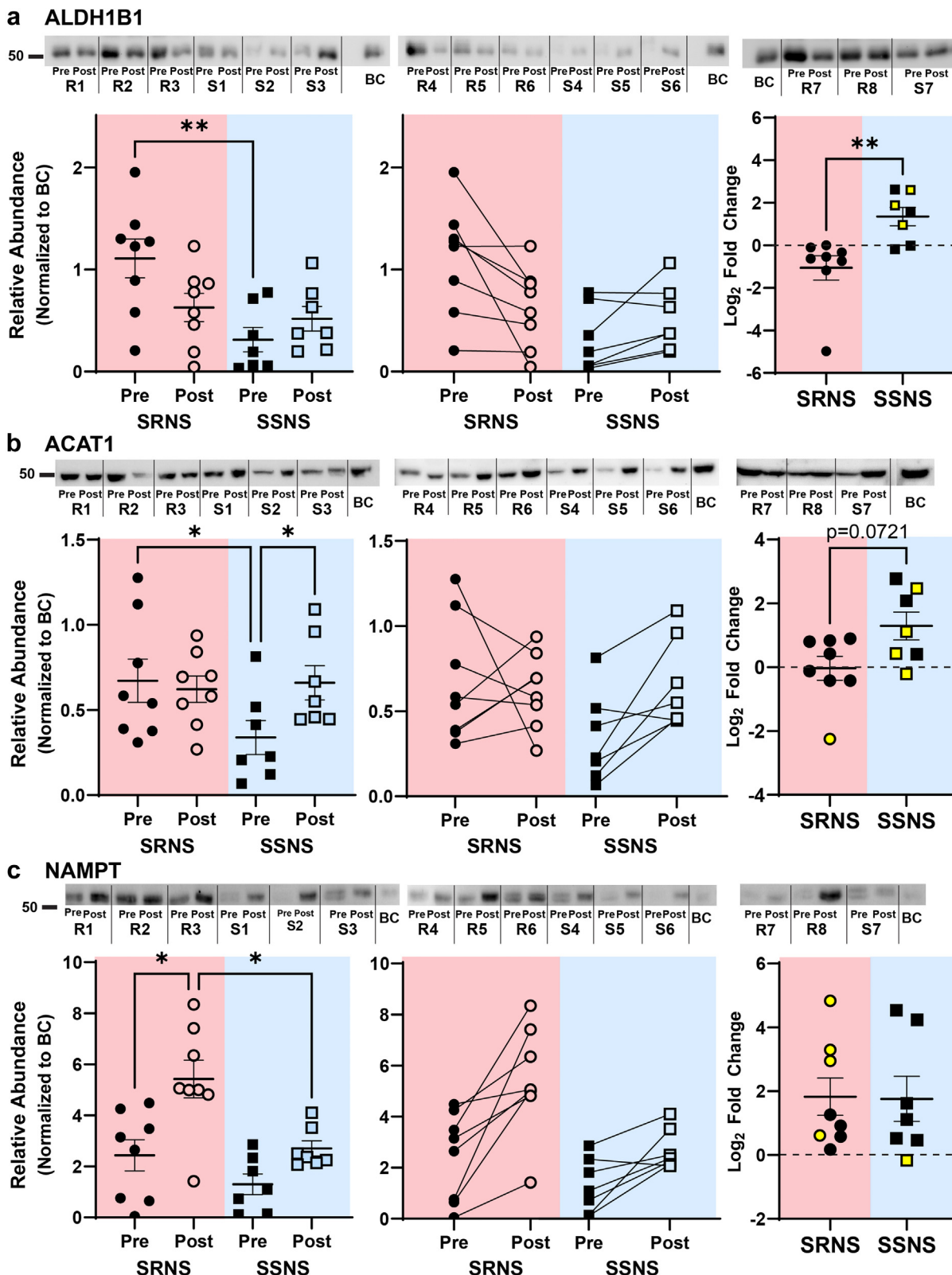


**Figure 7.** Validation of proteins-of-interest by integrated omics analysis using immunoblotting. Equal protein amounts of patient plasma were heat-denatured and subjected to immunoblotting. Images of bands of all samples are shown above their quantification and analysis for the respective proteins (ALDH1B1, ACAT1, and NAMPT). Bands were normalized to a corresponding blot control loaded to each blot, which was an identical sample of healthy adult plasma. (a) ALDH1B1, (b) ACAT1, and (c) NAMPT expression was examined before and after GC treatment. Graphs left to right show: (1) pretreatment and posttreatment relative abundances, (2) individual patient responses to GC treatment, and (3) the log<sub>2</sub> fold change of post/pre-ratio. Lines and whiskers on graphs represent mean ± standard error of the mean. Patients whose LFC trended similarly to that in Figure 5 are indicated with a yellow marker. Statistical significance was determined by Kruskal-Wallis (pre, post- levels) or Wilcoxon rank sum test (Log<sub>2</sub>FC), 2-tailed, with alpha = 0.05, as indicated \**P* < 0.05, \*\**P* < 0.01. SRNS, steroid resistant nephrotic syndrome; SSNS, steroid sensitive nephrotic syndrome.



Next, we analyzed ACAT1 protein expression and found that ACAT1 pre-GC levels were significantly ( $P < 0.05$ ) lower in patients with SSNS (Figure 7b, left panel), also demonstrating its potential as a predictive biomarker of SRNS. Patients with SSNS also had significantly ( $P < 0.05$ ) increased expression after GC treatment (Figure 7b, left panel), whereas SRNS patient responses were more heterogeneous (Figure 7b, left and middle panels). The  $\log_2$  fold change in ACAT1 expression with GC treatment showed a greater increase in SSNS versus SRNS, although the difference was not significantly significant ( $P = 0.0721$ ) (Figure 7b).

In addition, NAMPT was readily detected in patients' samples (Figure 7c), and NAMPT levels were significantly ( $P < 0.05$ ) increased in post-GC treated versus pre-GC treated patients (Figure 7c, left panel). Whereas patients with SSNS had a trend toward increased expression, the changes were not significant. Post-GC levels of NAMPT were significantly higher in patients with SRNS than in patients with SSNS ( $P < 0.05$ ) (Figure 7c, left panel), indicating its potential as a mechanistic biomarker of GC resistance.

## DISCUSSION

The lack of effective treatments for SRNS represents a major unmet medical need among both children and adults with NS and makes SRNS clinical management challenging. Available alternative immunosuppressants are incompletely effective and have significant side effects. Patients with SRNS also have an increased risk of progressive kidney failure. Therefore, there is a clear need to identify prognostic and predictive biomarkers that can prevent patients who present with SRNS from being unnecessarily treated with GC. Multiomics approaches have the potential to identify novel biomarkers, however, the analysis of such large datasets has historically been difficult. Although there are reports of proteomic and metabolomic profiles from the SRNS and SSNS, the heterogeneity between patients within the same clinical group can complicate the analysis of the datasets. The current studies were designed to use a novel "patient-specific" analytical approach that integrates proteomics and metabolomics data to understand the interplay of proteins and metabolites and to discover comprehensive pathways that differentiate SRNS from SSNS.<sup>18</sup> This approach of integrating different omics datasets from the same patient sample enabled both grouped analyses and personalized analyses for each patient. These studies confirm the ability of a novel "patient-specific" analytical approach to integrate disparate omics datasets to identify candidate biomarkers of SRNS not observed with either omics approach alone.

In these studies, we integrated proteomics and metabolomics data acquired from the plasma of children with SRNS and SSNS before and after GC treatment. We observed 34 significantly altered pathways in these patients. Using  $< -25\%$  or  $>25\%$  cutoffs for the Pathway Group Enrichment Index we narrowed the analysis to 12 pathways more frequently altered in SSNS and/or SRNS. We then narrowed our focus to the 5 most commonly regulated pathways hypothesizing that the most regulated pathways would be the most likely to contain changes in protein expression that could be confirmed by immunoblot. We found that nicotinate and nicotinamide metabolism and butanoate metabolism were more frequently activated in patients with SRNS than in patients with SSNS, whereas glycolysis or gluconeogenesis, mucin type O-glycan biosynthesis, and lysine metabolism were more frequently perturbed in patients with SSNS than in patients with SRNS. Quantitation of the molecules in these pathways identified NAMPT, NMNAT1, and SETMAR as more frequently altered in patients with SRNS than in patients with SSNS, whereas ALDH1B1, ACAT1, AASS, ENPP1, and pyruvate were more frequently perturbed in patients with SSNS than in patients with SRNS. Immunoblotting subsequently confirmed significant increases of NAMPT in patients with SRNS, and of ALDH1B1 and ACAT1 proteins in patients with SSNS. Pre-GC treatment plasma levels of ALDH1B1 and ACAT1, and post-GC treatment levels of NAMPT were significantly different between patients with SRNS and those with SSNS. These differences were present not only between groups but were also observed in individual patients who had that pathway identified in the "patient-specific" pathway analysis. These immunoblotting findings validated the pattern of expression of proteins associated with pathways identified in each group and were aligned with the patients within the group that had specific proteins upregulated or downregulated. The similar responses observed for ACAT1, ALDH1B1, and AASS (Figures 5, 6, 7), strongly suggest the involvement of the lysine metabolism pathway in steroid responsiveness in NS. Although these findings identified 2 new candidate molecular pathways (NAD<sup>+</sup> biosynthesis and lysine degradation) as potential regulators of clinical steroid resistance in children with NS, validation studies in a larger cohort of patients are needed.

Nephrology has entered the era of big data omic analysis through consortia such as the Kidney Precision Medicine Project, the Cure Glomerulonephropathy Consortium, and NEPTUNE.<sup>19-22</sup> With the RNA, protein, and metabolite profiling of kidney biopsy tissue and fluid samples, the need has arisen for effective computational tools and algorithms that can integrate

the varied high-dimensional profiling data to generate reliable biomarkers and identify disease mechanisms, and, ultimately, individualize treatment. Working toward an individualized approach, the current studies integrated available proteomics and metabolomics data to establish new protein-metabolite connectors that identify pathways relevant to either SSNS or SRNS. Using this approach, our underlying hypothesis that combining evidence from changes in both protein abundances and metabolite concentrations can improve our ability to identify the pathways involved in determining clinical steroid resistance versus steroid sensitivity was confirmed. This approach also enabled grouped as well as “patient-specific” analyses to better understand to what extent patients deviated within their groups.

Overall, the 5 pathways selected for further exploration were nicotinate and nicotinamide metabolism, butanoate metabolism (more frequently perturbed in patients with SRNS), lysine degradation, glycolysis or gluconeogenesis, and mucin type O-glycan biosynthesis (more frequently perturbed in patients with SSNS). Of note, nicotinate and nicotinamide metabolism (also known as  $\text{NAD}^+$  biosynthesis pathway) is involved in generating  $\text{NAD}^+$  and  $\text{NADP}^+$  via salvage pathways from nicotinamide.<sup>23</sup> In the kidney,  $\text{NAD}^+$  is known to stabilize mitochondrial function, and  $\text{NAD}^+$  depletion has been observed in acute kidney injury.<sup>24,25</sup> Increased intracellular and extracellular NAMPT levels are reported in conditions of acute or chronic inflammation and cancer.<sup>26-31</sup> In our studies, we found that patients with SRNS had significantly increased levels of plasma NAMPT after GC treatment compared to patients with SSNS. These findings suggest the hypothesis that an increase in NAMPT in patients with SRNS could contribute to GC resistance.

Notably, the lysine degradation pathway had multiple members (including AASS, ACAT1, and ALDH1B1) that were upregulated in patients with SSNS after successful GC treatment, in contrast to patients with SRNS in whom these levels failed to increase after GC treatment. These targets suggest a molecular mechanism that may either enable or induce remission of NS. In this context, the lysine degradation pathway may have direct clinical relevance, because defects causing reduced activity of its enzymes cause errors in metabolism.<sup>32</sup> In a notable study, treatment of mononuclear cells with the GC dexamethasone increased ACAT1 expression at both the mRNA and protein levels, with *in silico* analysis revealing a GC-response element in the *ACAT1* promoter.<sup>33</sup> Furthermore, ALDH enzymes have been shown to oxidize corticosteroids.<sup>34,35</sup> This suggests

the hypothesis that plasma ALDH preemptively degrades GCs and potentiates GC resistance. Our observation of higher plasma ALDH1B1 levels in patients with SRNS is consistent with this hypothesis. Upregulation of this pathway in response to GC might contribute to the clinical responsiveness to steroids in patients with SSNS.

These studies have several limitations and strengths. Most notably, our analyses were performed in a small number of metabolomic and proteomic datasets. We cannot generalize about the clinical utility of potential therapeutic targets and diagnostic biomarkers from our limited data. As such, the findings of selected specific molecular pathways and candidate biomarkers that differentiate SRNS from SSNS reported will require much larger validation studies that employ antibody-based methods. In addition, the methods employed in attempting to narrow the very large amounts of data derived from each patient studied necessitated the use of several mathematical cutoffs at key steps in the analyses. Because of an unequal number of patients in the SRNS and SSNS group, the Group Enrichment Index cutoff creates a calculation bias toward patients with SSNS as follows: if 2 more patients in the SSNS group as compared to the SRNS group have a pathway or molecule enriched, the index will be greater than 25% but it would take 3 more patients in the SRNS group as compared to the SSNS group for the index to be greater than 25%. These studies also had some important strengths in that this analysis was performed on specimens from NS patients both before GC treatment (i.e., steroid-naïve samples representing a “disease-only” state) and from those same patients following initial treatment with GC. In addition, the confirmation by immunoblot of findings only seen in merged proteomic and metabolomic data is a useful finding.

In summary, the current studies used a novel “patient-specific” approach to compare integrated plasma proteomic and metabolomic profiles from children with SSNS versus SRNS to identify predictive and mechanistic candidate biomarkers of SRNS. These studies highlight the potential of integrated plasma proteomics and metabolomics analyses to identify novel candidate biomarkers, and provide support for the evaluation of larger independent cohorts of patients with NS to confirm these and additional biomarkers of SRNS using orthogonal antibody-based assays such as enzyme-linked immunosorbent assay. Integrating omics data from patient blood, urine, and kidney biopsy samples may prove useful in advancing precision diagnostic and therapeutic approaches to kidney disease.

## APPENDIX

### List of the Pediatric Nephrology Research Consortium

Drs. John Mahan, Hiren Patel, and Richard F. Ransom (NCH, Columbus, OH)

Dr. Cynthia Pan (Medical College of Wisconsin, Milwaukee, WI)

Dr. Denis F. Geary (The Hospital for Sick Children, Toronto, ON, Canada)

Dr. Myra L. Chang (West Virginia University, Charleston, WV)

Dr. Keisha L. Gibson (University of North Carolina, Chapel Hill, NC)

Dr. Franca M. Iorember (Louisiana State University, New Orleans, LA)

Dr. Patrick D. Brophy (Children's Hospital, University of Iowa, Iowa City, IA)

Dr. Tarak Srivastava (Children's Mercy Hospital, Kansas City, MO)

Dr. Larry A. Greenbaum (Emory University School of Medicine, Atlanta, GA)

## DISCLOSURE

WES is a cofounder of NephKey Therapeutics, Inc; and is on the Board of Directors of NephCure Kidney International and receives no compensation as a member of the Board of Directors. LHM is on the academic advisory boards for Calliditas Therapeutics, Travers Therapeutics, and Reata Pharmaceuticals. All other authors declared no competing interests.

## ACKNOWLEDGMENTS

We thank the Pediatric Nephrology Research Consortium, its participating centers, physicians, study and nurse coordinators for their contributions toward the collection of the plasma samples used in this study. We also thank the Biopathology Core at NCH for storing and maintaining the sample biorepository. Finally, we thank the Ohio Supercomputer Center (OSC) for providing computing resources.

### Funding

WES and JBK were funded by NIDDK CureGN Ancillary R01 (DK 110077).

### Data Sharing Statement

Proteomics data was downloaded from MassIVE (<http://massive.ucsd.edu/>) data repository with the Center for Computational Mass Spectrometry at the University of California, San Diego (MSV000082114).

Metabolomics data was obtained from the NIH Common Fund's Data Repository and Coordinating Center (<http://www.metabolomicsworkbench.org>), with a Metabolomics Workbench Project ID: PR000648.

## AUTHOR CONTRIBUTIONS

Study design and conceptualization was done by SB, YZ, LL, and WES. The methodology was developed by YZ, SB, LL, and WES. The investigation was conducted by SB, YZ, MLM, TDC, JAD, YK, WP, SM, LL, and WES. Visualization was done by YZ, SB, MLM, TDC, JAD, WP, SM, LHM, SS, JBK, LL, and WES. Funding acquisition was done by JBK and WES. Manuscript preparation and editing was done by SB, YZ, MLM, TDC, JAD, YK, WP, SM, LHM, SS, JBK, LL, and WES.

## SUPPLEMENTARY MATERIALS

[Supplementary File \(PDF\)](#)

### Supplementary Methods.

**Figure S1.** Filtration process of proteomics data.

**Figure S2.** Log<sub>2</sub> fold change distributions of proteins and metabolites assists in the determination of cut-off values.

**Figure S3.** PCA plot of entire proteomic and metabolomic datasets alone.

**Figure S4.** Mapped proteins and metabolites in 2 altered pathways in SRNS patient R4.

**Figure S5.** Volcano plot based on the differential protein or metabolite expression (posttreatment vs. pretreatment) in SRNS versus SSNS.

**Table S1.** SRNS and SSNS pediatric patient demographics.

**Table S2.** Individual patient clinical data.

**Table S3.** Enriched KEGG pathways with hypergeometric *P*-value < 0.05 and their occurrence frequency in patients with SSNS and patients with SRNS.

**Table S4.** Downregulated KEGG pathways with hypergeometric *iP*-value < 0.05 and their occurrence frequency in patients with SSNS and patients with SRNS.

**Supplementary Data Files S1–S7.**

## REFERENCES

- Mace C, Chugh SS. Nephrotic syndrome: components, connections, and angiotensin-like 4-related therapeutics. *J Am Soc Nephrol.* 2014;25:2393–2398. <https://doi.org/10.1681/ASN.2014030267>
- Tapia C, Bashir K. *Nephrotic Syndrome.* StatPearls; 2022.
- Dumas De La Roque C, Prezelin-Reydit M, Vermorel A, et al. Idiopathic nephrotic syndrome: characteristics and identification of prognostic factors. *J Clin Med.* 2018;7:265. <https://doi.org/10.3390/jcm7090265>
- Zaorska K, Zawierucha P, Swierczewska M, Ostalska-Nowicka D, Zachwieja J, Nowicki M. Prediction of steroid resistance and steroid dependence in nephrotic syndrome children. *J Transl Med.* 2021;19:130. <https://doi.org/10.1186/s12967-021-02790-w>
- Hodson E. The management of idiopathic nephrotic syndrome in children. *Pediatr Drugs.* 2003;5:335–349. <https://doi.org/10.2165/00128072-200305050-00006>
- Agrawal S, Merchant ML, Kino J, et al. Predicting and defining steroid resistance in pediatric nephrotic syndrome

- using plasma proteomics. *Kidney Int Rep.* 2020;5:66–80. <https://doi.org/10.1016/j.ekir.2019.09.009>
7. Gooding JR, Agrawal S, McRitchie S, et al. Predicting and defining steroid resistance in pediatric nephrotic syndrome using plasma metabolomics. *Kidney Int Rep.* 2020;5:81–93. <https://doi.org/10.1016/j.ekir.2019.09.010>
  8. Li Q, Schissler AG, Gardeux V, et al. N-of-1-pathways Mix-Enrich: advancing precision medicine via single-subject analysis in discovering dynamic changes of transcriptomes. *BMC Med Genomics.* 2017;10(suppl 1):27. <https://doi.org/10.1186/s12920-017-0263-4>
  9. Vaske CJ, Benz SC, Sanborn JZ, et al. Inference of patient-specific pathway activities from multi-dimensional cancer genomics data using PARADIGM. *Bioinformatics.* 2010;26:i237–i245. <https://doi.org/10.1093/bioinformatics/btq182>
  10. Huang DW, Sherman BT, Tan Q, et al. The David Gene Functional Classification Tool: a novel biological module-centric algorithm to functionally analyze large gene lists. *Genome Biol.* 2007;8:R183. <https://doi.org/10.1186/gb-2007-8-9-r183>
  11. Zheng Q, Wang XJ. GOEAST: a web-based software toolkit for Gene Ontology enrichment analysis. *Nucleic Acids Res.* 2008;36:W358–W363. <https://doi.org/10.1093/nar/gkn276>
  12. Khatri P, Draghici S, Ostermeier GC, Krawetz SA. Profiling gene expression using onto-express. *Genomics.* 2002;79:266–270. <https://doi.org/10.1006/geno.2002.6698>
  13. Schussler-Fiorenza RSM, Contrepolis K, Moneghetti KJ, et al. A longitudinal big data approach for precision health. *Nat Med.* 2019;25:792–804. <https://doi.org/10.1038/s41591-019-0414-6>
  14. Stanberry L, Mias GI, Haynes W, Higdon R, Snyder M, Kolker E. Integrative analysis of longitudinal metabolomics data from a personal multi-omics profile. *Metabolites.* 2013;3:741–760. <https://doi.org/10.3390/metabo3030741>
  15. Rits IA. Declaration of Helsinki. Recommendations guidings doctors in clinical research. *World Med J.* 1964;11:281.
  16. Pang Z, Chong J, Li S, Xia J. MetaboAnalystR 3.0: toward an optimized workflow for global metabolomics. *Metabolites.* 2020;10. <https://doi.org/10.3390/metabo10050186>
  17. Sund R. Computer Age Statistical Inference: algorithms, Evidence, and Data Science Bradley Efron and Trevor Hastie Institute of Mathematical Statistics Monographs Cambridge University Press, 2016, (8th printing 2018), xix. *Int Stat Rev.* 2019;87:186–188. <https://doi.org/10.1111/insr.12320>
  18. Hansen J, Sealfon R, Menon R, et al. A reference tissue atlas for the human kidney. *Sci Adv.* 2022;8:eabn4965. <https://doi.org/10.1126/sciadv.abn4965>
  19. Saez-Rodriguez J, Rinschen MM, Floege J, Kramann R. Big science and big data in nephrology. *Kidney Int.* 2019;95:1326–1337. <https://doi.org/10.1016/j.kint.2018.11.048>
  20. El-Achkar TM, Eadon MT, Menon R, et al. A multimodal and integrated approach to interrogate human kidney biopsies with rigor and reproducibility: guidelines from the Kidney Precision Medicine Project. *Physiol Genomics.* 2021;53:1–11. <https://doi.org/10.1152/physiolgenomics.00104.2020>
  21. Mariani LH, Bomback AS, Canetta PA, et al. CureGN study rationale, design, and methods: establishing a large prospective observational study of glomerular disease. *Am J Kidney Dis.* 2019;73:218–229. <https://doi.org/10.1053/j.ajkd.2018.07.020>
  22. Gadegbeku CA, Gipson DS, Holzman LB, et al. Design of the Nephrotic Syndrome Study Network (NEPTUNE) to evaluate primary glomerular nephropathy by a multidisciplinary approach. *Kidney Int.* 2013;83:749–756. <https://doi.org/10.1038/ki.2012.428>
  23. Zapata-Perez R, Wanders RJA, van Karnebeek CDM, Houtkooper RH. NAD(+) homeostasis in human health and disease. *EMBO Mol Med.* 2021;13:e13943. <https://doi.org/10.15252/emmm.202113943>
  24. Poyan Mehr A, Tran MT, Ralto KM, et al. De novo NAD(+) biosynthetic impairment in acute kidney injury in humans. *Nat Med.* 2018;24:1351–1359. <https://doi.org/10.1038/s41591-018-0138-z>
  25. Ralto KM, Rhee EP, Parikh SM. NAD(+) homeostasis in renal health and disease. *Nat Rev Nephrol.* 2020;16:99–111. <https://doi.org/10.1038/s41581-019-0216-6>
  26. Audrito V, Messana VG, Deaglio S. NAMPT and NAPRT: two metabolic enzymes with key roles in inflammation. *Front Oncol.* 2020;10:358. <https://doi.org/10.3389/fonc.2020.00358>
  27. Neubauer K, Bednarz-Misa I, Walecka-Zacharska E, et al. Oversecretion and overexpression of nicotinamide phosphoribosyltransferase/pre-B colony-enhancing factor/visfatin in inflammatory bowel disease reflects the disease activity, severity of inflammatory response and hypoxia. *Int J Mol Sci.* 2019;20:166. <https://doi.org/10.3390/ijms20010166>
  28. Brentano F, Schorr O, Ospelt C, et al. Pre-B cell colony-enhancing factor/visfatin, a new marker of inflammation in rheumatoid arthritis with proinflammatory and matrix-degrading activities. *Arthritis Rheum.* 2007;56:2829–2839. <https://doi.org/10.1002/art.22833>
  29. Otero M, Lago R, Gomez R, et al. Changes in plasma levels of fat-derived hormones adiponectin, leptin, resistin and visfatin in patients with rheumatoid arthritis. *Ann Rheum Dis.* 2006;65:1198–1201. <https://doi.org/10.1136/ard.2005.046540>
  30. Nowell MA, Richards PJ, Fielding CA, et al. Regulation of pre-B cell colony-enhancing factor by STAT-3-dependent interleukin-6 trans-signaling: implications in the pathogenesis of rheumatoid arthritis. *Arthritis Rheum.* 2006;54:2084–2095. <https://doi.org/10.1002/art.21942>
  31. Jia SH, Li Y, Parodo J, et al. Pre-B cell colony-enhancing factor inhibits neutrophil apoptosis in experimental inflammation and clinical sepsis. *J Clin Invest.* 2004;113:1318–1327. <https://doi.org/10.1172/JCI19930>
  32. Leandro J, Houten SM. The lysine degradation pathway: subcellular compartmentalization and enzyme deficiencies. *Mol Genet Metab.* 2020;131:14–22. <https://doi.org/10.1016/j.ymgme.2020.07.010>
  33. Yang L, Yang JB, Chen J, et al. Enhancement of human ACAT1 gene expression to promote the macrophage-derived foam cell formation by dexamethasone. *Cell Res.* 2004;14:315–323. <https://doi.org/10.1038/sj.cr.7290231>
  34. Monder C, Purkaystha AR, Pietruszko R. Oxidation of the 17-aldol (20 beta hydroxy-21-aldehyde) intermediate of corticosteroid metabolism to hydroxy acids by homogeneous human liver aldehyde dehydrogenases. *J Steroid Biochem.* 1982;17:41–49. [https://doi.org/10.1016/0022-4731\(82\)90590-8](https://doi.org/10.1016/0022-4731(82)90590-8)
  35. Martin KO, Monder C. Oxidation of corticosteroids to steroid-21-oic acids by human liver enzyme. *Biochemistry.* 1976;15:576–582. <https://doi.org/10.1021/bi00648a019>